

ANL-6211
Chemistry - Separation
Processes for Plutonium
and Uranium
(TID-4500, 15th Ed.)
AEC Research and
Development Report

ARGONNE NATIONAL LABORATORY
9700 South Cass Avenue
Argonne, Illinois

NITRIDATION OF CRUCIBLE SKULLS FROM MELT REFINING

by

T. R. Johnson, G. F. Brunzie* and R. K. Steunenber

Chemical Engineering Division

September 1960

* Resident Student Associate

Operated by The University of Chicago
under
Contract W-31-109-eng-38

DISCLAIMER

This report was prepared as an account of work sponsored by an agency of the United States Government. Neither the United States Government nor any agency Thereof, nor any of their employees, makes any warranty, express or implied, or assumes any legal liability or responsibility for the accuracy, completeness, or usefulness of any information, apparatus, product, or process disclosed, or represents that its use would not infringe privately owned rights. Reference herein to any specific commercial product, process, or service by trade name, trademark, manufacturer, or otherwise does not necessarily constitute or imply its endorsement, recommendation, or favoring by the United States Government or any agency thereof. The views and opinions of authors expressed herein do not necessarily state or reflect those of the United States Government or any agency thereof.

DISCLAIMER

Portions of this document may be illegible in electronic image products. Images are produced from the best available original document.

TABLE OF CONTENTS

	<u>Page</u>
I. INTRODUCTION.	3
A. Description of EBR-II Fuel Cycle	3
B. Nitridation of Crucible Skulls	4
II. URANIUM-NITROGEN COMPOUNDS	5
III. EXPERIMENTAL PROCEDURE	5
A. Skull Preparation - Melt Refining	5
B. Skull Nitridation.	7
IV. EXPERIMENTAL RESULTS	8
A. Melt Refining.	8
B. Nitridation	9
V. DISCUSSION OF RESULTS	14
A. General	14
B. Compounds Formed	14
C. Correlation of Rates	15
VI. CONCLUSIONS.	15
ACKNOWLEDGEMENTS	17
BIBLIOGRAPHY.	17
APPENDIX: Mathematical Model of Gas-Solid Reactions Applied to the Nitridation of Crucible Skulls.	18

NITRIDATION OF CRUCIBLE SKULLS FROM MELT REFINING

by

T. R. Johnson, G. F. Brunzie and R. K. Steunenber

I. INTRODUCTION

A. Description of EBR-II Fuel Cycle

Discharged fuel from the Experimental Breeder Reactor (EBR-II) will be reprocessed by melting the uranium alloy in a zirconia crucible.⁽¹⁾ This "melt refining" process removes fission products (except for the noble metals) by volatilization, slagging, or reaction with the crucible walls. The elements more noble than uranium (zirconium, niobium, molybdenum, technetium, ruthenium, rhodium, palladium, silver, and tin) remaining in the uranium may be beneficial alloying metals. To prevent their excessive buildup in fuel recycled to the reactor several times, a small fraction (5 to 10 per cent) of the fuel will be removed in each pass and replaced with pure uranium. The uranium-bearing material remaining in the crucible after melt refining, the crucible "skull," serves as this "dragout stream." The amount of skull formed approximates the percentage dragout required to produce useful alloys. For the EBR-II fuel cycle, a liquid-metal process is being developed to recover purified uranium from the crucible skull. The equilibrium concentrations of noble metals in the fuel will depend on the burnup and the fraction of dragout material per pass. Table 1⁽²⁾ shows the equilibrium concentrations of the noble metals based on 2 per cent burnup and 5 per cent dragout per pass. The alloy composition chosen for the first core loading of the reactor is also shown. These alloys of uranium or plutonium with their fission products are called "fissium" alloys.

The pyrometallurgical operations for the EBR-II reactor will be carried out remotely in the argon annulus of the Fuel Cycle Facility. The argon atmosphere in this shielded operating cell will be continuously purified from oxygen and water. The nitrogen content will be controlled by periodically adding pure argon to the cell. The maximum concentrations of impurities expected in the cell atmosphere are:

oxygen:	< 100 ppm
water:	< 10 ppm
nitrogen:	< 5 v/o.

Table 1

EBR-II FUEL COMPOSITION

Element	Equilibrium Fuel Composition (2% Total Atoms Fissioned and 5% Dragout Per Pass)	
	(w/o)	Selected Initial Fuel Composition (w/o)
Zr	0.3a	0.1
Nb	0.01 ^a	0.01
Mo	3.4	2.5
Ru	2.6	1.9
Tc	1.0	-
Rh	0.5	0.3
Pd	0.3	0.2
U ²³⁵	46.0	47.5
U ²³⁸	42.8	47.5
Pu ²³⁹	3.2	-

^a Based on 50 per cent zirconium and niobium removal during melt refining by slagging with carbon.

B. Nitridation of Crucible Skulls

It is known that nitrogen reacts rapidly with uranium at temperatures above 400 C.⁽³⁾ Due to heating by fission products, the estimated temperature of the melt refining crucible skull will be between 400 and 1000 C. These skulls may be exposed to the cell atmosphere for several days as they await processing. The amount of reaction between the skulls and the low-pressure nitrogen and the effects of the reaction on the crucible and skull are important considerations to the design of the liquid-metal dragout process. Experimental work, for example, has indicated that nitrated fissium is not readily reduced by magnesium in zinc solutions.⁽⁴⁾

The temperature and nitrogen partial pressure to which the skulls will be subjected depend on many factors which cannot be evaluated at the present time. If the crucibles and skulls are partially covered or if they are stored near one another, their temperatures may become very high (~1000 C). Even if they are left exposed, their temperatures may be high enough to cause rapid reaction with nitrogen.⁽⁴⁾ It may prove impractical

to keep the nitrogen content of the cell at a very low value or to seal the crucibles completely against the cell atmosphere.

The range of variables chosen for this study were: temperature, 400 to 800 C; pressure, 8 to 76 mm Hg. These conditions should span those met in practice. The effect of zirconium content was investigated by using fissium alloys containing 2.8 weight per cent and less than 0.05 weight per cent zirconium. The percentages of the other alloying elements and the melt refining conditions were not varied significantly.

II. URANIUM-NITROGEN COMPOUNDS

Several compounds in the nitrogen-uranium system have been reported,⁽³⁾ but only UN, U₂N₃ and UN₂ can be considered stoichiometric. Compounds having a lower nitrogen content than the mononitride are considered to be solutions of the mononitride in the metal. A two-phase region exists between UN and U₂N₃. Compositions between U₂N₃ and UN₂ are single-phase. A gradual change in the crystal structure occurs between U₂N₃ and UN₂.

Direct nitridation of uranium metal below 1300 C proceeds directly to a nitride with a composition between U₂N₃ and UN₂ without forming UN as an intermediate. The composition depends on the temperature and nitrogen pressure. Above 1300 C, the higher nitrides decompose to UN.

The higher nitrides are partially reduced by hydrogen at temperatures above 100 C with the formation of ammonia. The nitrides are easily oxidized to uranium oxides by oxygen at low temperatures (~200 C).

III. EXPERIMENTAL PROCEDURE

A. Skull Preparation - Melt Refining

To simplify the experiment and yet to simulate the actual process condition, cerium was substituted for the rare earths and yttrium, and a single set of typical conditions for melt refining were employed. A fissium alloy ingot (300 to 500 grams) and a freshly cut, shiny piece of cerium metal were melted together in a zirconia crucible in an induction furnace. The amount of cerium added (0.6 w/o) was equivalent to the total amount of all rare earths and yttrium present in a fissium fuel at 2 per cent burnup.

The crucibles were dry-pressed zirconia, stabilized with 5 per cent calcium oxide (Norton mixture Z300 SP), of dimensions: 2 in. OD, 4 in. outside height, $1\frac{3}{8}$ in. ID, $3\frac{1}{2}$ in. deep. The crucibles were degassed at 1200 C and 0.01 micron for six hours before use. The arrangement of the induction

furnace is shown in Figure 1. This furnace has been described previously.⁽⁵⁾ The vacuum pumps were capable of maintaining a vacuum of less than 0.1 micron.

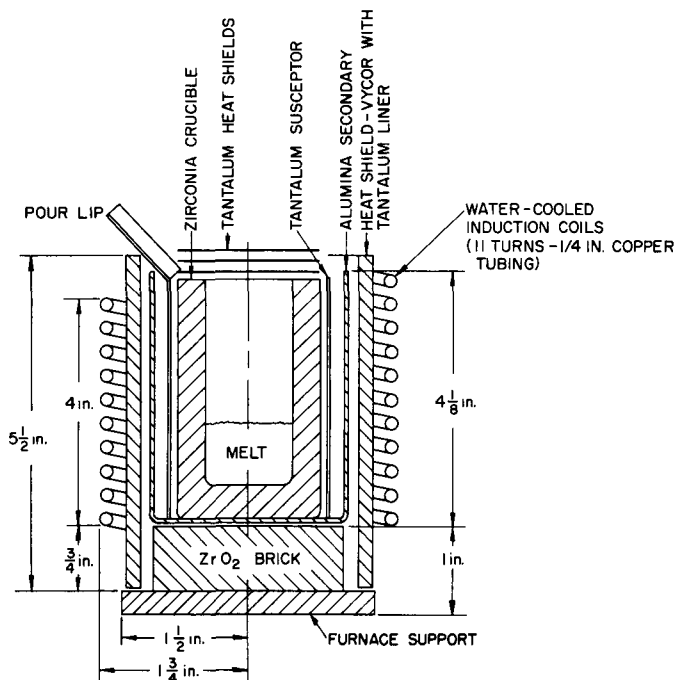


Figure 1
INDUCTION FURNACE FOR MELT REFINING

After the charge had been placed in the furnace, the system was evacuated to less than 3×10^{-4} mm. The charge was heated to 700 C for an initial degassing period of 30 minutes. About 650 mm of helium, purified by passing it through an activated carbon trap at liquid nitrogen temperature, were then added to the furnace. The charge temperature was raised to 1350 ± 25 C at a heating rate of about 30 C/min. The temperature was measured with an optical pyrometer by sighting on the melt surface through a hole in the tantalum heat shields. A correction of +30 C applied to the pyrometer reading was required to compensate for the emissivity of the molten metal and the transmittance of the optical flat.

The melt was held at 1350 C for two hours, then poured into a copper mold without interruption of the power. The ingot cast from one run was used as the alloy charge for the next. The furnace and crucible were allowed to cool to room temperature before air was admitted.

The approximate compositions of the two fissium alloys prepared for the nitridation studies are shown in Table 2.

Table 2

COMPOSITION OF FISSIUM ALLOYS
USED FOR NITRIDATION STUDIES

<u>Element</u>	<u>High-zirconium Alloy (w/o)</u>	<u>Low-zirconium Alloy (w/o)</u>
Zr	2.8	< 0.05
Mo	2.7	2.74
Ru	2.7	2.08
Pd	0.6	0.54
U	Balance	Balance

B. Procedure for Nitriding

The apparatus for nitridation of the crucible skulls consisted of a resistance-heated stainless steel furnace tube and a manifold for measurement of gas volume (Figure 2). The tube and manifold were leak-tested and their volumes were calibrated. The temperature of the furnace was measured by a central chromel-alumel thermocouple in a well extending to within one inch of the bottom of the crucible. This thermocouple was calibrated at the melting points of cadmium and magnesium with an accuracy of ± 3 C. Uniform temperature control of the crucible was achieved by controlling the outside temperature of the furnace tube. The crucible temperature did not fluctuate more than ± 5 C.

Before the run was started, the gas-metering tank was first evacuated, then charged with about 400 mm of nitrogen directly from a cylinder. The crucible was placed in the furnace tube, the tube was closed, evacuated (< 0.1 mm), and heated to the desired temperature. The reaction was started by adding nitrogen from the metering tank to raise the furnace pressure to the required level. The reaction was slow enough to enable manual control of the pressure with an accuracy of ± 2 mm. The rate of the reaction was determined from readings of the metering tank pressure.

The experiment was terminated when the nitrogen absorption became too slow to follow (~ 0.02 millimol of nitrogen/minute). The furnace was evacuated and allowed to cool before the crucible was removed.

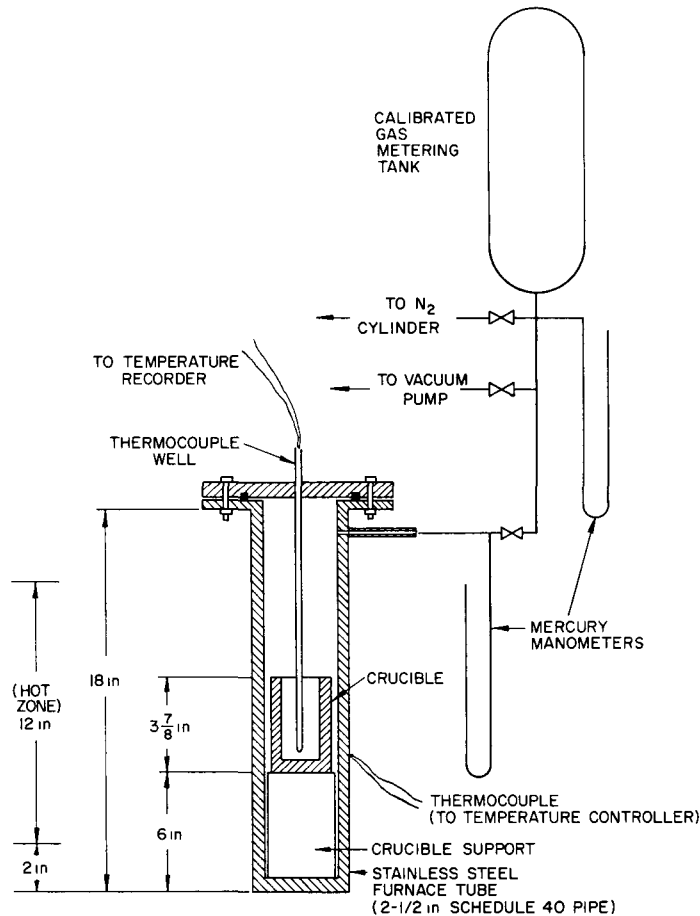


Figure 2
EXPERIMENTAL EQUIPMENT FOR
SKULL NITRIDATIONS

IV. EXPERIMENTAL RESULTS

A. Melt Refining

During melt refining, cerium is removed preferentially from uranium by reaction with the zirconia crucible. The reaction appears to produce a lower oxide of zirconium⁽⁶⁾ since there is no increase in zirconium content in the poured ingot. The cerium removal from the poured metal was greater than 95 per cent and averaged 97 per cent in all cases in which analyses were obtained. Recoveries of poured metal ranged between 85 and 95 per cent.

The degree of transfer of uranium from the ingot into the skull was slightly greater than that of the noble metals. This effect is shown to be small by the increase in noble metal concentration as the fissium alloy

is remelted several times. After ten melt-refining cycles the concentrations of all noble metals, except zirconium, had increased by approximately 9 per cent of their original concentrations (e.g., from 6.0 to 6.54 w/o). Within the precision of the analytical procedure, the zirconium concentration was constant.

The material remaining in the crucible after pouring is the crucible "skull." It consisted of metal (the "button") and a uniform, shiny black reaction layer (the "dross") tightly adhering to the crucible. The crucible walls, normally a light yellow color, were completely blackened to a height corresponding to the level of the molten charge.

B. Nitridation

The experimental conditions and results are summarized in Table 3 and in Figures 3, 4, 5, 6, and 7.

Table 3

SUMMARY OF NITRIDATION RUNS

Run No.	Total Charge Weight (g)	Skull Weight (g)	Dross Weight (g)	Mols U in Dross (g-mols)	Furnace Temp (C)	Nitrogen Pressure (mm Hg)	Skull Area (sq cm)
<u>High-zirconium Alloy</u>							
805	330	18.6	10.4	0.032	700	8	31
803	382	19.4	14.3	0.046	800	8	34.5
807	298	23.2	13.4	0.045	800	8	29
731	412	28.7	13.9	0.044	500	38	36.5
724	432	17.9	12.6	0.039	600	38	38
722	462	26.5	19.6	0.063	700	38	40
717	253	21.2	11.8	0.040	800	38	26
713 ^a	281	21.0	11.0	0.036	400	76	28
714	254	21.7	10.0	0.018	500	76	26
710	357	22.0	11.0	0.037	600	76	33
804	357	27.1	14.0	0.046	700	76	33
713 ^a	281	21.0	11.0	0.036	700	76	28
709	312	15.0	13.0	0.043	800	76	30
<u>Low-zirconium Alloy</u>							
902	412	24.9	14.8	0.049	600	8	36.5
903	387	18.6	10.1	0.031	700	8	35
904	367	28.6	13.0	0.043	800	8	33.5
826	547	29.8	15.1	0.047	500	38	45.5
827	517	25.7	14.6	0.046	600	38	43.5
831	463	24.4	15.1	0.049	700	38	40
828	487	24.2	15.0	0.048	800	38	41.5
820	702	43.8	30.5	0.105	500	76	56
821 ^b	659	31.1	21.2	0.069	600	76	53
824 ^b	627	45.8	21.2	0.070	700	76	51
825	582	35.4	19.3	0.063	800	76	48

^a No reaction at 400 C, skull re-used at 700 C.

^b Crucible broke.

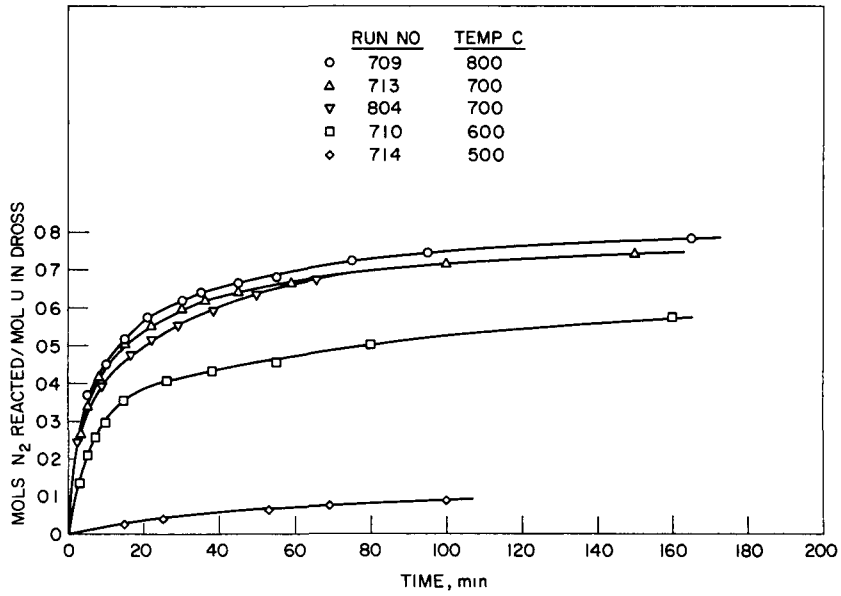


Figure 3
 NITRIDATION OF FISSIUM CRUCIBLE DROSS
 Nitrogen Pressure: 76 mm Hg
 Zirconium Content: 2.8 w/o

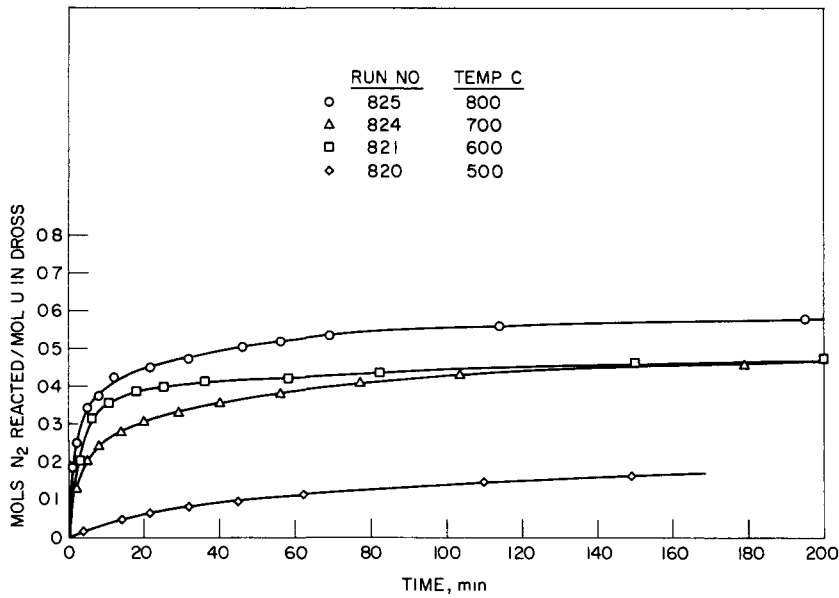


Figure 4
 NITRIDATION OF FISSIUM CRUCIBLE SKULLS
 Nitrogen Pressure: 76 mm Hg
 Zirconium Content: <0.05 w/o

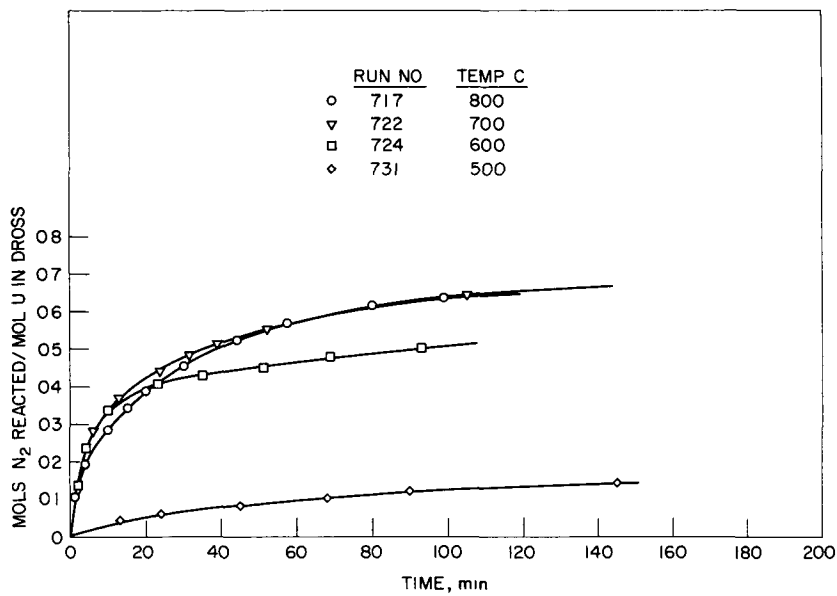


Figure 5
 NITRIDATION OF FISSION CRUCIBLE DROSS
 Nitrogen Pressure: 38 mm Hg
 Zirconium Content: 2.8 w/o

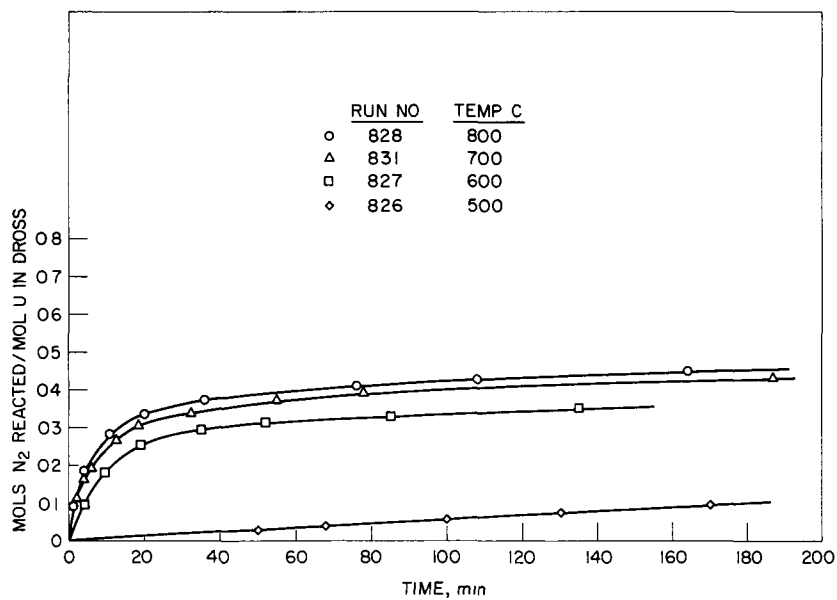


Figure 6
 NITRIDATION OF FISSION CRUCIBLE SKULLS
 Nitrogen Pressure: 38 mm Hg
 Zirconium Content: <0.05 w/o

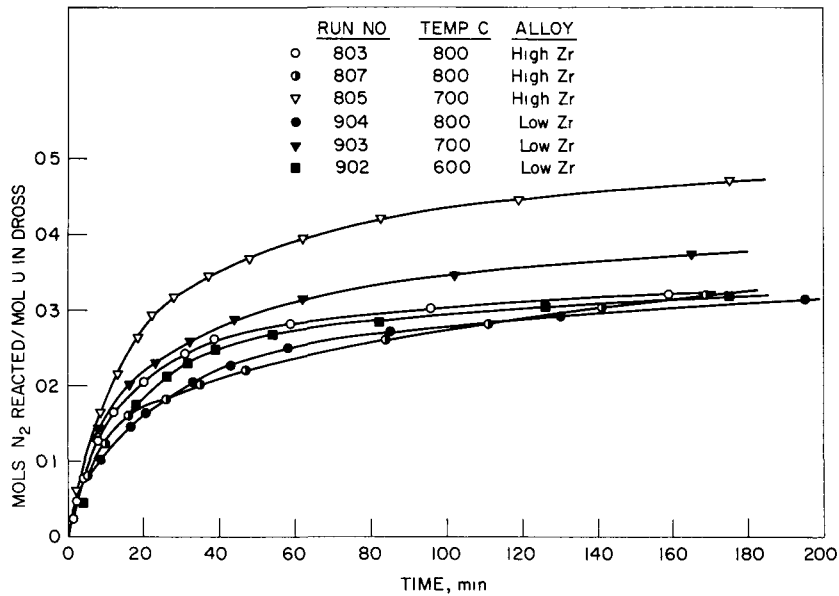


Figure 7
 NITRIDATION OF FISSIUM CRUCIBLE SKULLS
 Nitrogen Pressure: 8 mm Hg
 Zirconium Content: 2.8 w/o & 0.5 w/o

The ordinates of the reaction curves were calculated by the following method:

(1) It was assumed that the massive metallic button did not react significantly with the nitrogen. Even at the highest temperature and pressure there was no visible evidence of any reaction other than a slight discoloration of the metal surface. This was confirmed by a separate experiment in which a 16-gram piece of fissium metal gained less than one per cent in weight in four hours at 750 C under a nitrogen pressure of 75 mm Hg.

(2) The weight of the skull was determined by weighing the degassed crucible before and after melt refining.

(3) The metallic button which had been separated from the crucible and dross by nitridation was weighed separately. The initial weight of the dross was found by subtracting the weight of the button from the initial skull weight.

(4) The number of moles of uranium in the dross was calculated by the equation

$$\text{Mols U} = \left[\frac{(\text{Initial Wt of Dross}) - (0.97)(\text{Wt of Ce Charged})}{238} \right] \times (\text{Wt Fraction of U in Alloy})$$

The value 0.97 represents the average extent of cerium removal from the ingot during melt refining. In those cases in which a total dross analysis was obtained, the calculated value of the number of moles of uranium agreed within 10 per cent of the value estimated from the chemical analysis.

(5) The number of moles of nitrogen absorbed was calculated from the pressure drop in the calibrated metering tank. The amount of nitrogen added to fill the furnace tube initially was negligible except in the runs at 500 C and 76 mm Hg. A correction was made in these runs.

(6) It was experimentally verified that the rate of nitrogen absorption by the stainless steel and by the zirconia crucible was negligible.

(7) The superficial skull area was calculated from the depth of the melt and the crucible dimensions.

In the majority of runs the zirconia crucible was intact after melt refining and nitridation. The nitrided dross was usually finely powdered and had fallen to the bottom of the crucible. The dross and button could be easily and cleanly poured from the crucible. Typical particle size distributions of the nitrided dross, after burning in air, are shown in Table 4.

Table 4

<u>SCREEN ANALYSES OF TYPICAL NITRIDED DROSSES</u>							
Run No.	804	820	821	824	825	827	831
Alloy	High Zr	Low Zr	Low Zr	Low Zr	Low Zr	Low Zr	Low Zr
Furnace Temp (C)	700	500	600	700	800	600	700
Nitrogen Pressure (mm)	76	76	76	76	76	38	38
Screen Analysis (mesh)							
>60	58.9	56.2	61.0	76.9	50.1	52.0	59.8
60-100	17.8	7.9	17.8	10.1	17.4	12.7	23.1
100-200	12.5	9.5	13.3	6.7	13.5	20.5	8.1
200-325	4.9	10.6	4.5	3.0	8.4	8.3	4.1
<325	5.1	15.4	2.7	2.2	9.7	5.6	3.4

Many of the nitrated skulls were pyrophoric. Upon exposure to air, the powdered dross immediately began to burn at a barely perceptible red heat. A strong odor of ammonia, probably due to reaction of the nitrides with water vapor in the air, was detected.

V. DISCUSSION OF RESULTS

A. General

The rate of reaction between the crucible dross and nitrogen increased with temperature and pressure except at low pressures. At the lowest nitrogen pressure used (8 mm Hg), the rates at 800 C and 600 C were significantly slower than at 700 C. The high-zirconium alloy (2.8 w/o) reacted faster than did the low-zirconium alloy (less than 0.05 w/o). The reaction rate at 400 C and 76 mm Hg was too low to be measured with the apparatus used.

The reaction rate was determined with undiluted nitrogen at pressures corresponding to the anticipated partial pressure of nitrogen in the argon atmosphere of the Fuel Cycle Facility. Mixtures of nitrogen and argon were not used because of experimental complications. The presence of argon would affect the reaction rate in two ways: it would offer a diffusion barrier for nitrogen and act as a heat transfer medium to remove the heat of reaction. Because the nitridation reaction is relatively slow, gas-phase diffusion cannot be an important rate-controlling step. With regard to heat loss, the principal mechanism at the experimental temperatures is radiation. The calculated heat generation rate of the reaction is not large enough to raise the surface temperature more than 50 C. No temperature rises in excess of 30 C were noted during the experiments. However, there was considerable lag in the central thermocouple of the apparatus. The reaction rate is not influenced appreciably by temperatures above 600 C. Therefore the presence of argon should not greatly influence the reaction rate.

B. Compounds Formed

The ratio of moles of nitrogen consumed to moles of uranium in the dross seems to approach an approximate limit between 0.7 and 0.8, which corresponds roughly to U_2N_3 . In X-ray diffraction analyses of two nitrated skulls (Runs 713 and 710) which did not seem to be pyrophoric, uranium, UN, ZrO_2 , ZrN were detected as minor components. A major component had the structure of uranium dinitride, but $Ce_2O_3 \cdot 2ZrO_2$ (a probable product of melt refining) has a similar crystal structure. Furthermore, the U_2N_3 structure can be considered⁽⁷⁾ as a distorted UN_2 crystal with nitrogen atoms missing in a regular pattern. In the phase region between U_2N_3 and UN_2 , there is no definite phase change.

Data⁽³⁾ on the equilibrium pressure of nitrogen over uranium-nitrogen solid phases indicate that UN_2 formation under the experimental conditions would be unlikely. In the temperature range from 500 to 800 C, the decomposition pressure of UN_x increases rapidly as x increases above 1.5. The pressure of nitrogen over UN_x at 492 C is 50 mm for $x=1.65$ and 825 mm for $x=1.68$. It was concluded that the uranium could nitride completely to a nitride above U_2N_3 , but not as far as the dinitride.

C. Correlation of Rates

Correlation of the data by several different methods was attempted. In other work, the parabolic rate law has been used to express the nitridation rate of uranium. An effort was made to apply this, as well as the other common rate laws (linear, cubic and logarithmic), but none was satisfactory. These rate laws ordinarily imply a constant reaction area. In this case, however, the reaction area very probably changes as the reaction proceeds. Therefore, one would expect a rate expression to contain explicitly the mass of unreacted solid.

A mathematical model was derived in which it was assumed that the reaction took place on the surface of a small spherical particle and that the product adhered to the reacting particle. After an initial period, the reaction rate was considered to be controlled by gaseous diffusion through the shell of reacted solid. The initial reaction rate appeared to be controlled by some other mechanism; for the model, adsorption of the gas on the particle surface was chosen as the rate-controlling step.

By making several approximations and treating the constants as empirical coefficients, the derived equation was applied to the data obtained on the nitridation rate of melt refining skulls. Although the correlation was not entirely successful, it proved to be the best of the several methods tried and provided a reasonable method of scaling up the data to larger skulls. It should be emphasized that the mathematical treatment is intended to be only a correlation of the experimental data and not an indication or proof of any particular mechanism for the reaction.

The mathematical model is presented in the Appendix.

VI. CONCLUSIONS

Low-pressure nitrogen reacts readily with melt-refining skulls, forming nonstoichiometric U_2N_3 . The skull is pulverized and is loosened from the crucible by the reaction. The nitrated product is very pyrophoric in air at room temperature. The reaction of nitrogen with the metallic button is much slower. The dross reacts first, falling off the crucible wall, covering the metallic button and partially protecting it from attack by

nitrogen. Nitridation of the metallic button may be important for hot skulls exposed to nitrogen for times in excess of a few hours. It has been reported⁽⁹⁾ that fissium alloy nitrides at a rate comparable to that of pure uranium.

The reaction of the dross with nitrogen was significant at 500 C and 38 mm Hg nitrogen pressure and at 600 C and 8 mm Hg. The reaction probably takes place at 400 C and 8 mm Hg, but it was too slow to follow with the apparatus used. At higher temperatures and pressures, the reaction with the dross was nearly complete in two or three hours. The reaction rate was not greatly increased by temperatures above 700 C.

The components present in the skull are not well known, but it may be assumed that nitrogen reacts with fissium metal particles that are occluded in the dross. A correlation based on the reaction of the gas with many small spherical particles seems to fit the data reasonably well (see Appendix). The reaction rate per mol of uranium present is then independent of the total mass of the dross and of the superficial surface area. The total reaction rate (g-mol per minute) is therefore a linear function of the quantity of material, indicating that the reaction curves in Figures 3, 4, 5, 6 and 7 can be applied directly to larger skulls.

Possible nitridation of the skulls in the EBR-II Fuel Cycle Facility may have some effect on the design of the reprocessing plant. The temperature rise of the skull due to the reaction with low-pressure nitrogen will not be large - less than 50 C for less than thirty minutes. Scavenging of the atmosphere in the argon annulus of the Facility by the skull will not be significant compared to the estimated leak rate of 0.01 cu ft of air per minute into the cell.

Cracks often develop in the full-scale crucibles after melt refining. The crucible is then held together largely by the strength of the adhering skull. If the skull nitrides significantly, it will be pulverized and may allow the crucible to fall apart.

For the purposes of the dragout process, it must be assumed that fully nitrided skulls will have to be handled in the EBR-II fuel reprocessing plant, since the temperature of the crucible, nitrogen content of the argon atmosphere, and the manner and duration of storage of the crucibles after melt refining have not yet been determined. The first step of the contemplated dragout process is a direct oxidation of the crucible skull to separate the skull and crucible, to pulverize the skull, and to prepare a material amenable to processing in a liquid metal system. The oxidation of the nitrided uranium should present no difficulties.

ACKNOWLEDGEMENTS

The authors wish to acknowledge the suggestions, support and interest of Dr. R. C. Vogel, Dr. H. M. Feder, Mr. L. Burris, Jr, and Dr. L. Leibowitz. Thanks are also extended to Mr. R. L. Christensen, who assisted with the experimental work, Mr. D. S. Flikkema, who performed the X-ray analyses, and Mrs. G. Kesser, who provided advice and assistance with the chemical analyses.

BIBLIOGRAPHY

1. Burris, L., et al., Developments in Melt Refining of Reactor Fuels, Proceedings of the Second International Conference on the Peaceful Uses of Atomic Energy, United Nations, Geneva (1958) Vol. 17, p. 401.
2. Burris, L., et al., The Melt Refining of Irradiated Uranium: Application to EBR-II Fast Reactor Fuel. I. Introduction, Nuclear Sci. and Eng., 6, 493 (1959).
3. Katz, J. J. and Rabinowitch, E., The Chemistry of Uranium, National Nuclear Energy Series, Vol. VIII, No. 5, McGraw-Hill Book Co., New York (1951), p. 232.
4. Pierce, R. D., Private Communication.
5. Bernstein, G. J., et al., The Melt Refining of Irradiated Uranium: Application to EBR-II Fast Reactor Fuel. II. Experimental Furnaces, Nuclear Sci. and Eng., 6, 496 (1959).
6. Rosen, C. L., Chellew, N. R. and Feder, H. M., The Melt Refining of Irradiated Uranium: Application to EBR-II Fast Reactor Fuel. IV. Interaction of Uranium and its Alloys with Refractory Oxides, Nuclear Sci. and Eng., 6, 504 (1959).
7. Rundle, R. E., et al., The Structures of the Carbides, Nitrides and Oxides of Uranium, J. Am. Chem. Soc., 70, 99 (1948).
8. Adda, Y., Étude Cinétique de l'Oxydation, de la Nituration et de l'Hydrogenation de l'Uranium, CEA-757 (AEC-tr-3749)(1958).
9. Schnizlein, J. G., Private Communication.
10. Low, M. J. D., Kinetics of Chemisorption of Gases on Solids, Chem. Rev., 60, 267 (1960).

Appendix: Mathematical Model of Gas-Solid Reactions Applied to Nitridation of Crucible Skulls

Consider a single spherical particle of radius R . The reaction takes place at a radius r , which varies as the reaction proceeds. The gas must diffuse through the reaction layer of thickness $R - r$. Let:

- s = moles of solid reacted (g-moles/particle)
 $A(r)$ = area of reacting surface (sq cm)
 $A(R)$ = surface area of particle (sq cm)
 A_M = mean area for diffusion (sq cm)
 ρ = molar density of the solid (g-moles/cc)
 B = permeability of reacted solid (g-moles/(min)(cm)(atm))
 K_R = surface reaction rate constant (g-moles/(min)(sq cm)(atm))
 K_A = surface adsorption rate constant (g-moles/(min)(sq cm)(atm^{1/2}))
 p = bulk gas pressure (atm)
 p^* = interfacial gas pressure at the reacting surface (atm)

The various rates may be expressed as follows:

Reaction at the metal interface:

$$\frac{ds}{dt} = K_R A(r) p^* \quad (1)$$

Adsorption (neglecting surface saturation effects):⁽¹⁰⁾

$$= K_A A(R) p^{1/2} \quad (2)$$

Diffusion through the reacted solid

$$= \frac{BA_M}{R - r} (p - p^*) \quad (3)$$

Assuming that diffusion is the rate-controlling step and that

$$A_M = 4\pi Rr \text{ (i.e., the geometric mean),} \quad (4)$$

then

$$\frac{ds}{dt} = \frac{4\pi BRrp}{R - r} \quad \text{if } p^* \ll p. \quad (5)$$

Also,

$$ds = -\rho A(r)dr = -4\pi\rho r^2 dr \quad (6)$$

$$s = -\int_R^r 4\pi\rho r^2 dr = \frac{4}{3}\pi\rho(R^3 - r^3) \quad (7)$$

$$r = R\left(1 - \frac{3s}{4\pi\rho R^3}\right)^{1/3} \quad (8)$$

Substituting for r in (5),

$$\frac{ds}{dt} = \frac{4\pi BpR\left(1 - \frac{3s}{4\pi\rho R^3}\right)^{1/3}}{1 - \left(1 - \frac{3s}{4\pi\rho R^3}\right)^{1/3}} \quad (9)$$

Let m be the fraction of the solid particle reacted:

$$m = 3s/4\pi\rho R^3 \quad (10)$$

Written in the dimension of time alone, (9) becomes

$$\frac{dm}{dt} = \frac{3Bp}{\rho R^2} \frac{(1-m)^{1/3}}{1 - (1-m)^{1/3}} \quad (11)$$

In the initial stages of the reaction, the diffusion rate would not be expected to be the rate-controlling step. If it is assumed, instead, that the initial rate-controlling step is the adsorption rate of the gas on the solid, the law may be represented by the equation

$$\frac{ds}{dt} = K_A A(R)p^{1/2} \quad (12)$$

Since $A(R) = 4\pi R^2$,

$$\frac{ds}{dt} = 4\pi K_A R^2 p^{1/2} \quad (13)$$

Assuming that a time t_T can be chosen at which diffusion becomes the rate-controlling step, the rate expressions can be integrated independently:

$$\int_0^{t_T} \left(\frac{ds}{dt}\right) dt = s_T = 4\pi K_A R^2 p^{1/2} t_T \quad (14)$$

and

$$\int_{s_T}^s \left[\left(1 - \frac{3s}{4\pi\rho R^3} \right)^{-1/3} - 1 \right] ds = \int_{t_T}^t 4\pi BRp dt, \quad (15)$$

which becomes

$$2\pi\rho R^3 \left[\left(1 - \frac{3s_T}{4\pi\rho R^3} \right)^{2/3} - \left(1 - \frac{3s}{4\pi\rho R^3} \right)^{2/3} \right] + (s_T - s) = 4\pi BRp(t - t_T) \quad (16)$$

Using (14) to eliminate t_T from (16), and writing in dimensionless form,

$$\left(1 - m_T \right)^{2/3} + \frac{2}{3} m_T \left(1 + \frac{p^{1/2} B}{R K_A} \right) - (1 - m)^{2/3} - \frac{2}{3} m = \frac{2Bpt}{\rho R^2} \quad (17)$$

where

$$m_T = 3s_T / 4\pi\rho R^3$$

Let:

$$f(m) = 1 - (1 - m)^{2/3} - \frac{2}{3} m \quad (18)$$

Then (17) becomes

$$f(m) - f(m_T) + \left(\frac{2}{3} m_T \right) \left(\frac{Bp^{1/2}}{R K_A} \right) = \left(\frac{2Bp}{\rho R^2} \right) t \quad (19)$$

where, if $t > t_T$, m_T and $f(m_T)$ are constants.

Several approximations must be made in order to apply this model to the nitridation of crucible skulls. For a bed containing particles of various sizes, the rate expressions can be integrated or summed over all particles. Screen analyses of the nitrated product are probably not indicative of the reaction area. Furthermore, the particles may not be spherical. Since there is a density difference between uranium metal and the nitride, the diffusion distance in equation (3) is not exactly represented by $(R - r)$ and it cannot be corrected by a simple function.

As an approximation, it is assumed that R is an average effective radius of all particles, whether or not they are actually spherical. Then equations (9) and (10) can be extended directly to the entire bed of reacting particles. Equation (19) is then written as

$$f(m) - f(m_T) + \frac{2}{3} C_1 p^{1/2} m_T = C_2 pt \quad (20)$$

where m_T , C_1 and C_2 are treated as empirical coefficients.

A correlation of the data obtained with the high-zirconium alloy is shown in Figures 8 and 9. It was assumed that U_2N_3 was the final reaction product. The value of C_2p can be determined from the slopes of the upper sections of the curves. An isothermal plot (Figure 10) of C_2p versus p , the nitrogen pressure, gives straight lines of slope C_2 . At $t = 0$,

$$C_1 p^{1/2} = \frac{f(m_T) - f(m)_{t=0}}{\frac{2}{3} m_T}$$

Values of m_T are obtained from breaks in the curves of Figures 8 and 9, and $f(m)_{t=0}$ is obtained from the ordinate intercept as in Figure 11.

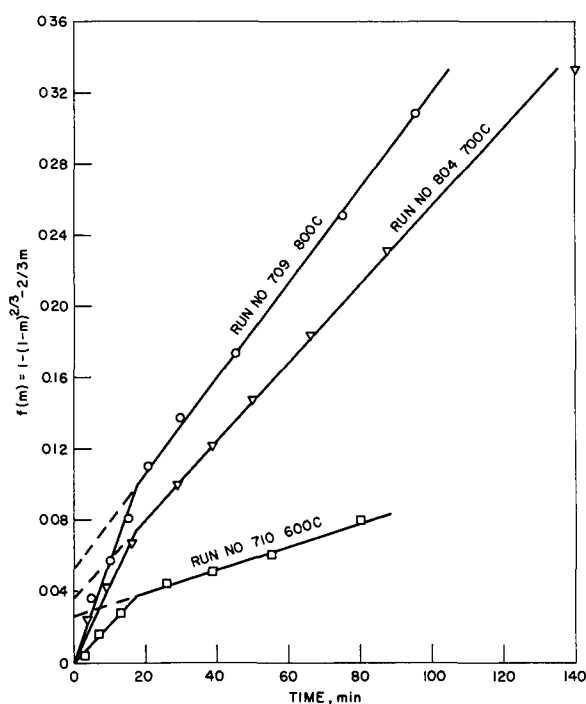


Figure 8

VARIATION OF $f(m)$ WITH TIME

(NITROGEN PRESSURE: 76 mm Hg
ZIRCONIUM CONTENT: 2.8 w/o)

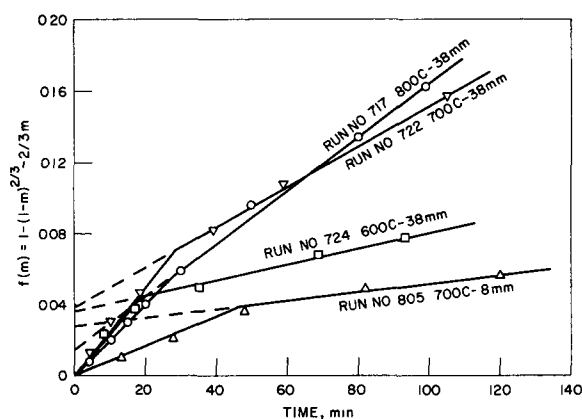


Figure 9

VARIATION OF $f(m)$ WITH TIME

(NITROGEN PRESSURE: 38 and
8 mm Hg
ZIRCONIUM CONTENT: 2.8 w/o)

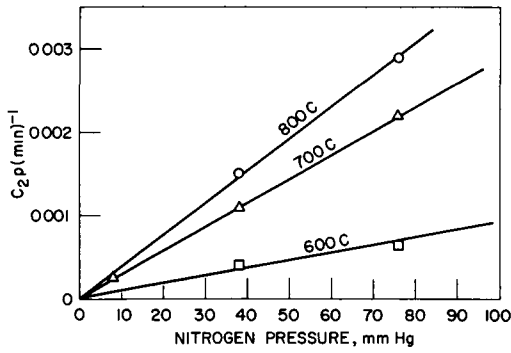


Figure 10

VARIATION OF C_2p WITH NITROGEN PRESSURE, p , AND TEMPERATURE

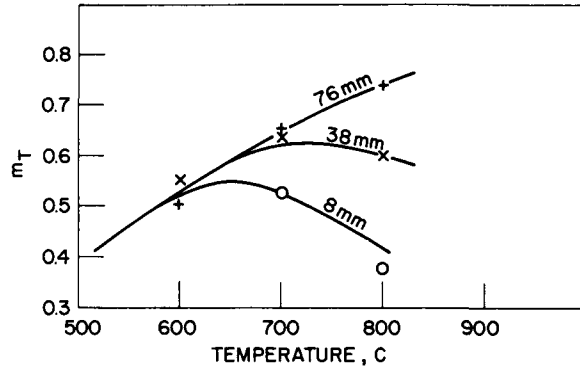


Figure 11

VARIATION OF m_T WITH TEMPERATURE AND PRESSURE

The values of $C_1p^{1/2}$ are plotted against $p^{1/2}$ in Figure 12. Straight lines were drawn through the points from which C_1 was calculated. Figure 13 shows generally the dependence of C_1 and C_2 on temperature. It is interesting to note that the ratio C_2/C_1 is nearly constant (Table 5).

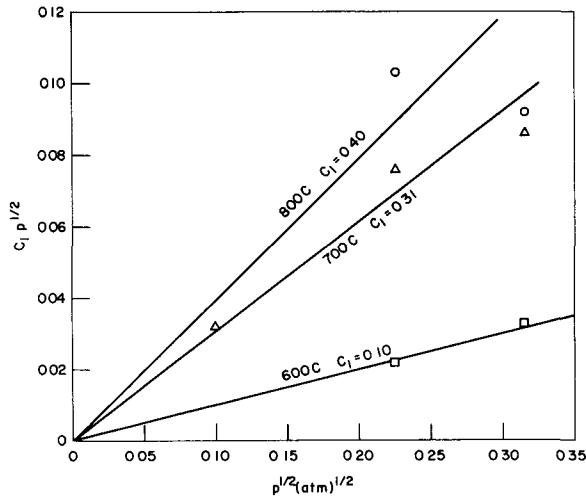


Figure 12

VARIATION OF $C_1p^{1/2}$ WITH $p^{1/2}$ AND TEMPERATURE

Figure 13

CORRELATION OF C_1 AND C_2 WITH TEMPERATURE

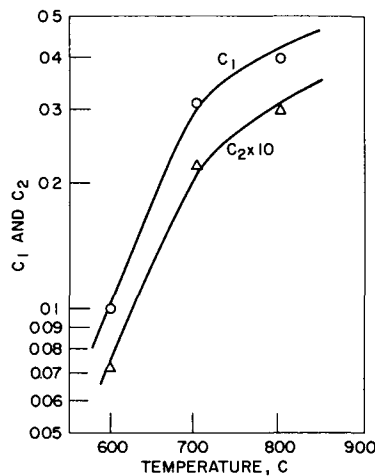


Table 5

EXPERIMENTAL PARAMETERS

Temp (C)	Nitrogen Pressure (mm Hg)	$f(m_T)$	$f(m)_{t=0}$	m_T	$C_1 p^{1/2}$	$C_2 p$ (min) ⁻¹
700	8	0.039	0.028	0.514	0.032	0.00024
600	38	0.047	0.039	0.554	0.022	0.00041
700	38	0.072	0.039	0.653	0.076	0.0011
800	38	0.056	0.015	0.596	0.103	0.0015
600	76	0.037	0.026	0.502	0.033	0.00064
700	76	0.074	0.036	0.660	0.086	0.0022
800	76	0.098	0.053	0.734	0.092	0.0029

Temp (C)	C_1 (atm) ^{-1/2}	C_2 (atm) ⁻¹ (min) ⁻¹	C_2/C_1 (atm) ^{-1/2} (min) ⁻¹
600	0.10	0.0072	0.072
700	0.31	0.022	0.072
800	0.40	0.030	0.075